

Article

Human Management Decreased Suspended Particle Size in the Loess Plateau Rivers during the 1980s to the 2010s

Keyu Li ¹, Dong Liu ^{2,*}, Zhiqiang Qiu ¹, Mengwei Duan ³, Xiaodao Wei ⁴ and Hongtao Duan ^{1,2,5,*}

¹ College of Urban and Environment Sciences, Northwest University, Xi'an 710127, China; likeyu@stumail.nwu.edu.cn (K.L.); 202210263@stumail.nwu.edu.cn (Z.Q.)

² Key Laboratory of Watershed Geographic Sciences, Nanjing Institute of Geography and Limnology, Chinese Academy of Sciences, Nanjing 210008, China

³ School of Transportation and Geomatics Engineering, Shenyang Jianzhu University, Shenyang 110168, China; mengweiduan@stu.sjzu.edu.cn

⁴ Shanghai Investigation, Design & Research Institute Co., Ltd., Shanghai 200050, China; weixiaodao@sidri.com

⁵ Shaanxi Key Laboratory of Earth Surface System and Environmental Carrying Capacity, Northwest University, Xi'an 710127, China

* Correspondence: dliu@niglas.ac.cn (D.L.); htduan@nwu.edu.cn (H.D.)

Abstract: The study of river sediment is a broad and complex field. One of the very important parameters is suspended particle size (SPS), which is indispensable for understanding water–sediment dynamics. As one of the most serious soil erosion areas in the world, the Loess Plateau delivers a large amount of sediment to the Yellow River and its numerous tributaries. Studies on riverine SPS in the Loess Plateau have received extensive attention. In this study, we investigate the spatiotemporal variations of SPS in the Loess Plateau rivers and analyze the driving factors along with their relative importance. Through the analysis of SPS data from 62 hydrological stations, the results indicated the spatial distribution of SPS was similar in the 1980s and 2010s, with both coarser particles mainly distributed in the northern rivers and finer particles mainly distributed in the southern rivers. During the 1980s to the 2010s, the mean SPS on the Loess Plateau decreased from 33 μm to 20 μm , with mean reductions of 42.0%, 29.4%, 46.3%, and 36.8% in the northern, western, southwestern, and southeastern basins, respectively. The most significant changes in SPS were observed in the Kuye, Wuding and Jalu River basins in the northern region, with decreases ranging from 27 to 73 μm . In the 1980s, topography (slope) and human management, followed by precipitation, were the key factors affecting SPS variability, contributing 25.7%, 25.9% and 24.0%, respectively. In the 2010s, the explanatory power of topographic slope on SPS variability declined by 16.6%, and other natural factors no longer significantly influenced SPS variability. The results of this study can serve as a reference for integrated basin management and sustainable ecosystem development in river catchments around the world.

Keywords: driving forces; human management; Loess Plateau; particle size; variation



Citation: Li, K.; Liu, D.; Qiu, Z.; Duan, M.; Wei, X.; Duan, H. Human Management Decreased Suspended Particle Size in the Loess Plateau Rivers during the 1980s to the 2010s. *Sustainability* **2024**, *16*, 799. <https://doi.org/10.3390/su16020799>

Academic Editor: Fernando António Leal Pacheco

Received: 4 December 2023

Revised: 4 January 2024

Accepted: 14 January 2024

Published: 17 January 2024



Copyright: © 2024 by the authors. Licensee MDPI, Basel, Switzerland. This article is an open access article distributed under the terms and conditions of the Creative Commons Attribution (CC BY) license (<https://creativecommons.org/licenses/by/4.0/>).

1. Introduction

Suspended sediment indicates granular materials such as soil, rock, organic matter, and other solid particles in the water column and is an important component of aquatic ecosystems [1]. The sources of suspended sediment in rivers are diverse, including soil erosion, bank failure, streambed sediment resuspension, and human activities like mining and stream channelization [2]. Suspended particle size (SPS) is one of the basic physical properties of suspended sediment. Analyzing SPS in rivers is beneficial for understanding the dynamic environmental conditions and sediment transport patterns within basins and for deepening the understanding of water and sediment movement [3]. SPS significantly affects the riverine transport of pollutants (nutrients, heavy metals, and organics) and is crucial in controlling riverine and estuarine geomorphological and biological processes [4].

Thus, the study of SPS variations in rivers can provide significant value for ecological conservation, environmental management, and sustainable ecosystem development of the basins.

Riverine SPS shows highly spatiotemporal dynamic characteristics, and these spatiotemporal variations show great diversity and complexity. For example, for rivers in the Humber and Tweed basins in the United Kingdom, Walling et al. [5] found that there were obvious spatial variations in SPS across different rivers, even within a basin. For the Mississippi River in the United States, D'Sa et al. [6] found that the SPS was highly influenced by river flow, sediment resuspension, and coastal ocean circulation. For the Yangtze River in China, Guo et al. [7] found that the SPS varied along with both seasons and locations and was closely related to human activities. The high dynamism of SPS necessitates comprehensive monitoring and in-depth research to better comprehend and manage the variability of SPS in global rivers, particularly in the context of current global climate change and increasing human activity.

Riverine SPS is jointly determined by natural factors (topography, climate, hydrology) and human activities within basins. These factors influence SPS by affecting soil erosion intensity and river flow velocity [8]. Geographical factors such as topography determine the sediment source, thereby influencing the SPS [9]. Climate changes can result in alterations in flood frequency and precipitation patterns, subsequently affecting the transport and distribution of suspended sediment with varying particle sizes [10]. Anthropogenic factors such as land use changes, soil and water conservation measures, and urbanization can also affect the SPS [11]. Changes in land use can potentially expose soil, resulting in an increased input of fine sediment [12]. Soil and water conservation affect SPS by attenuating soil erosion and sediment inputs [13]. Moreover, the impacts of all factors change spatiotemporally.

Although several other studies have mentioned how drivers influence SPS variability, such as topography [14], human activities [15] and climate change [16], quantitative information on the relative importance of the different factors is still very limited, and therefore, further investigations are needed to identify and quantify them. In addition, the study of river sediment is a broad and complex field, and significant spatial variations in particle size distribution may exist among different rivers or even different locations within the same river [17]. The Loess Plateau, one of the world's highest sediment-producing regions, has more than 200 rivers originating from it. The Yellow River, which has the highest sediment content in the world, flows through the Loess Plateau. Therefore, more research is needed to gain a deeper understanding of the spatial pattern of the SPS, the temporal change trends, and the influencing mechanisms within such a large-scale river system to fill the gap in the existing research.

In view of this, the aim of this study is to investigate the long-term spatial and temporal variations in SPS in the Loess Plateau rivers and the influencing factors within a 30-year time span. The specific objectives are: (1) to analyze the spatiotemporal variation characteristics of SPS in different rivers of the Loess Plateau during the 1980s and 2010s; (2) to quantify the contributions of various driving factors to the spatial variability of SPS in each period; (3) to determine the relative changes in the importance of different factors affecting SPS over the two periods. This study is significant for soil and water conservation, environmental protection, and ecological engineering construction in the Loess Plateau and other river basins globally.

2. Study Area

The Loess Plateau covers an area of approximately 640,000 km² (33°41' N–41°16' N; 100°52' E–114°33' E) and is located in the northwestern part of China (Figure 1). The annual average temperature is approximately 4.3 °C in the northwest region of the Loess Plateau and about 14.3 °C in the southeast [18]. Precipitation across the Loess Plateau exhibits a highly uneven spatial pattern, with annual rainfall ranging from 450 to 720 mm [19]. The Loess Plateau is predominantly covered by a layer of loess (100–300 m depth), has a

relatively low vegetation coverage, and is characterized by a globally recognized hotspot for soil erosion [18]. The Chinese government implemented a series of measures in the Loess Plateau to address soil erosion and protect the ecological environment that has been ongoing since the 1980s. These measures include optimizing land use, constructing terraces, carrying out reforestation and grassland restoration, implementing land retirement and forest closure, and building reservoirs [20]. The Loess Plateau is also rich in natural resources (petroleum, natural gas, and coal) and a significant economic production region in China.

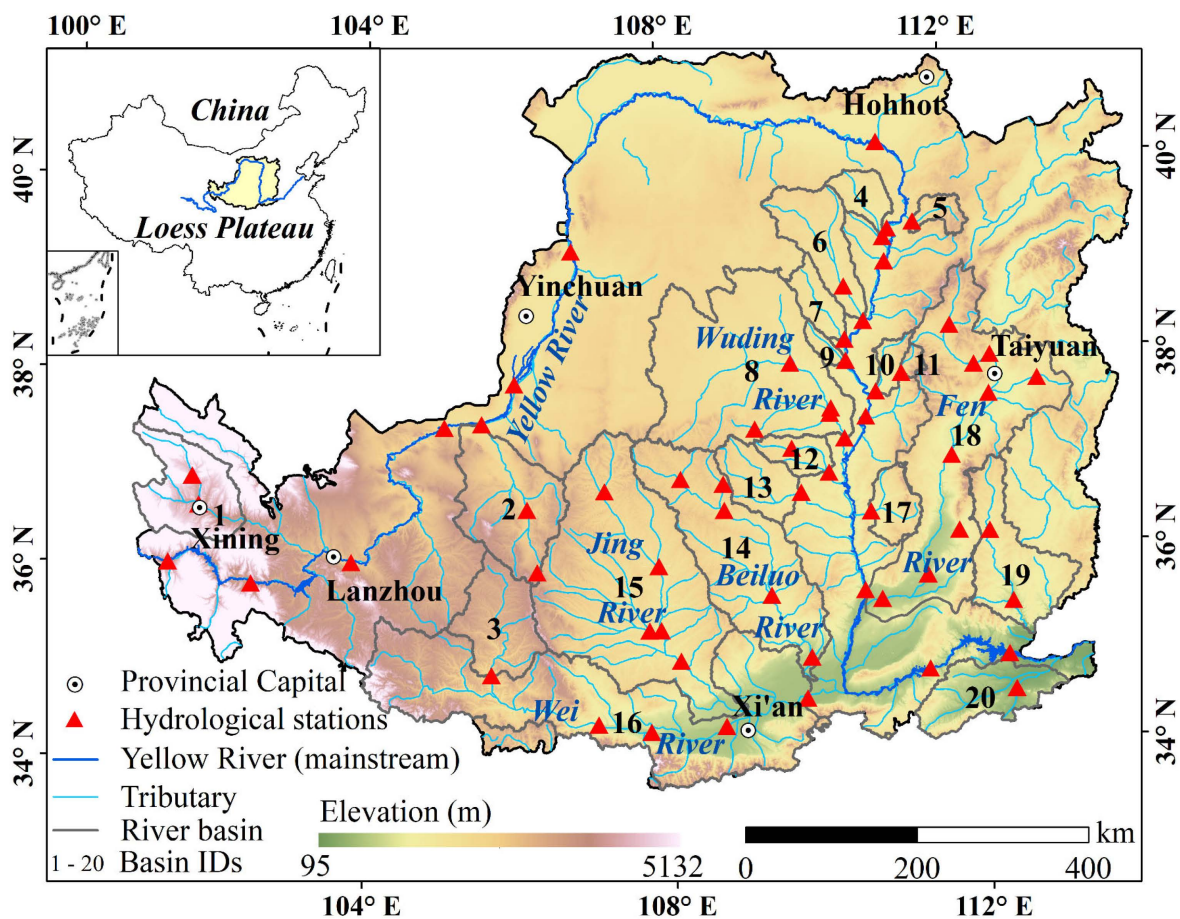


Figure 1. The Loess Plateau and the hydrological stations ($N = 62$). The digital elevation model was sourced from <http://loess.geodata.cn> (accessed on 1 March 2023). Please refer to Table 1 for detailed information about different river basins.

Bounded by the Loess Plateau, the Yellow River originates from the Qinghai-Tibet Plateau, flows northward, traverses the Hetuo Plain, then turns southward, and finally flows eastward into the ocean (Figure 1). The river network system of the Loess Plateau predominantly revolves around the Yellow River, covering a vast expanse and spanning multiple provinces in China. In the Loess Plateau region, there are approximately 32 significant tributaries flowing into the Yellow River. These tributaries are crucial in suspended sediment and water discharge sources. Some of the prominent tributaries include the Wei River, Jing River, Fen River, Kuye River, Yan River, Wuding River, Beiluo River, and Tuwei River (Figure 1). Generally, the topographies of these tributary basins exhibit a west-to-east descending pattern.

Table 1. The statistical information about different river basins. NDVI—normalized difference vegetation index; Temp.—air temperature (°C); Pre.—annual total precipitation (mm/yr); Pop.—population density (person/km²). W—western part; N—northern part; SW—southwestern part; SE—southeastern part.

No.	River Name	Regions	Stations	NDVI	Changes during the 1980s to the 2010s			SPS
					Temp.	Pre.	Pop.	
1	Huangshui River	W	2	0.08	1.47	29.46	58	−8
2	Qingshui River	W	3	0.10	1.33	64.89	15	−2
3	Hulu River	W	1	0.09	1.34	54.30	4	−7
4	Huangfu River	N	1	0.07	1.29	81.48	16	−12
5	Pianguan River	N	1	0.1	1.15	90.16	5	2
6	Kuye River	N	2	0.12	1.41	96.79	46	−54
7	Tuwei River	N	1	0.15	1.29	138.72	21	−9
8	Wuding River	N	5	0.13	1.25	97.10	7	−28
9	Jialu River	N	1	0.19	1.14	157.37	2	−36
10	Qiushui River	N	1	0.15	0.94	119.88	32	−13
11	Beichuan River	N	1	0.08	0.98	94.19	17	−10
12	Qingjian River	SW	2	0.19	0.90	55.84	1	−13
13	Yan River	SW	1	0.14	0.92	54.17	29	−12
14	Beiluo River	SW	5	0.07	1.03	32.67	12	−18
15	Jing River	SW	5	0.10	1.05	53.62	14	−7
16	Wei River	SW	4	0.08	1.31	7.47	49	−13
17	Xinshui River	SE	1	0.10	0.87	58.23	12	−11
18	Fen River	SE	9	0.08	1.13	32.22	92	−4
19	Qin River	SE	2	0.06	1.02	7.68	40	−16
20	Yi River	SE	1	0.06	1.03	−49.41	119	0
21	Yellow River	/	13	/	/	/	/	/

3. Materials and Methods

3.1. Suspended Particle Size Data

To investigate the spatiotemporal variations of SPS in the Loess Plateau rivers during the 1980s and 2010s, monthly mean SPS data at 62 hydrological stations for the years 1978–1982 and 2008–2012 were utilized. Among these 62 hydrological stations, SPS data were absent for one station in the 1980s and for six stations in the 2010s. These data were sourced from the Loess Plateau SubCenter (<http://loess.geodata.cn> (accessed on 20 December 2022)) and cover various sandy and coarse sandy tributaries in the middle and lower reaches of the Yellow River. Specifically, 13 stations were located along the main course of the Yellow River, while the remaining 49 stations were situated along its tributaries (Figure 1). Annual median particle size data for 14 hydrological stations for 2018–2022 from the Yellow River Sediment Bulletin published by the Yellow River Conservancy Commission (YRCC).

The measurement of SPS involved field sampling followed by laboratory analysis. In the 1980s, laboratory analysis primarily employed sieving or photometric counting methods. The sieve analysis method required basic equipment such as sieving tubes, samplers, washing sieves, balance, thermometer, sand receiver, tailings settling cup, electric drying oven, glass drying dish, and stopwatch. The main instrument used for photometric counting was the DLY-95A photoelectric particle analyzer [21]. However, in the 2010s, more advanced laser analysis techniques became widely adopted, and the instrument mainly used for measurements was the Malvern Mastersizer 2000 [22]. Based on the monthly data, this study computed the arithmetic mean SPS values for different stations in the 1980s and 2010s, and the mean SPS for each basin across the two periods.

We also obtained the SPS distribution data at the 54 hydrological stations except for the SPS data. SPS distribution data represents the volume percentage smaller than a particular particle size. The particle size classes include 2, 4, 8, 16, 31, 62, and 125 μm . Similar to the

SPS data, we calculated the mean SPS distribution at different hydrological stations in the 1980s and the 2010s.

3.2. Basin Boundary Delineation

The Loess Plateau covers a vast area characterized by significant spatial variations in topography, meteorological conditions, and other factors. These disparities contribute to a pronounced variability in SPS across river basins. To compare SPS in different river basins, this study employed the Automatic Outlet Relocation (AOR) algorithm proposed by Xie et al. [23] to delineate the watershed boundaries of different Yellow River tributaries (Figure 1, Table 1). The AOR algorithm can efficiently relocate outlets and correct the river network by analyzing the cumulative flow gradient along the river network's flow direction, providing a rapid way to establish a river basin without the need for manual intervention. To be specific, based on the spatial distribution of hydrological stations along the Yellow River, we initially identified the geographical locations of outlets for 20 Yellow River tributaries. Subsequently, using the software with a graphical user interface provided by Xie et al. [23], we delineated the basin boundaries. The number of hydrological stations within each delineated basin is shown in Table 1.

3.3. Multi-Source Products

Multi-source data were used to investigate the driving factors behind the spatiotemporal variation of SPS in the Loess Plateau. SRTM DEM data were obtained from NASA (<https://www.earthdata.nasa.gov/> (accessed on 1 March 2023)) at a spatial resolution of 30 m. Data on precipitation, air temperature, NDVI, LULC, and population density were obtained from the Resource and Environmental Science Data Center (<http://www.resdc.cn/> (accessed on 9 June 2023)). The precipitation and air temperature data (1 km) represent the spatially interpolated annual averages for the 1980s and 2010s [24]. The NDVI data were derived from the Global Inventory Modeling and Mapping Studies (8 km) and covered the time periods of 1981–1982 and 2008–2012 [25]. The LULC data were produced by the Institute of Geographic Sciences and Natural Resources Research, Chinese Academy of Sciences, using Landsat satellite images (30 m) and covered the years 1980 and 2010 [26]. Population density data (1 km) for the 1990s and 2010s were generated by the Institute of Geographic Sciences and Natural Resources Research, Chinese Academy of Sciences, using LULC, nighttime light intensity, and investigated population density [27]. Due to inconsistencies in data resolution and spatial reference information, we processed the data using the ArcGIS 10.4 software. All the above data were projected in UTM zone 50 of the northern hemisphere with WGS 84 datum and re-sampled to 1000-by-1000 m pixel size for co-registration.

For the various data mentioned above, this study calculated the mean values for different sub-basins of the Yellow River tributaries (Table 1). Moreover, the DEM data were applied to calculate the slope and aspect, and their mean values were computed for sub-basins. The land use data were reclassified into six types: cropland (paddy field, dry land), forest (shrubbery, sparse forest land, and woodland), grassland (low, medium, and high coverage grassland), water bodies (river and canals, lake, reservoir and pond, permanent glacier snow land, and mudflat), impervious (urban land, rural settlement, other construction land), and unused land (sand, gobi, saline-alkali soil, swampy land, bare land, naked rock). Subsequently, the proportions of cropland area in different sub-basins were calculated. The results for different data in the 1980s and 2010s are depicted in Figure 2.

3.4. Statistical Methods

Correlation analyses were performed to determine the statistical relationships between SPS and human management, slope and precipitation. The adjusted determination coefficients (R^2) of the regression equations were used to reflect each factor's explanatory power and determine the relative importance of different affecting factors. Moreover, a one-way analysis of variance (ANOVA) was performed to assess the influence of the land use types

on SPS. In addition, descriptive statistical analyses were used to determine the variation trend and variability of the SPS, with indicators including mean, minimum, maximum, standard deviation, and coefficient of variation (CV). The CV is defined as follows [28]:

$$CV = \sqrt{\frac{\sum_{i=1}^n (X_i - \bar{X})^2}{n}} / \left(\frac{X_1 + X_2 + \dots + X_n}{n} \right) \quad (1)$$

In the equation, σ represents the standard deviation; \bar{X} represents the mean; n is the total sample number; X_1, X_2, \dots, X_n denote the sampled data. For all the aforementioned statistics, the significance level $p < 0.01$ (2-tailed test) indicates an extremely significant correlation, and $p < 0.05$ indicates a significant correlation.

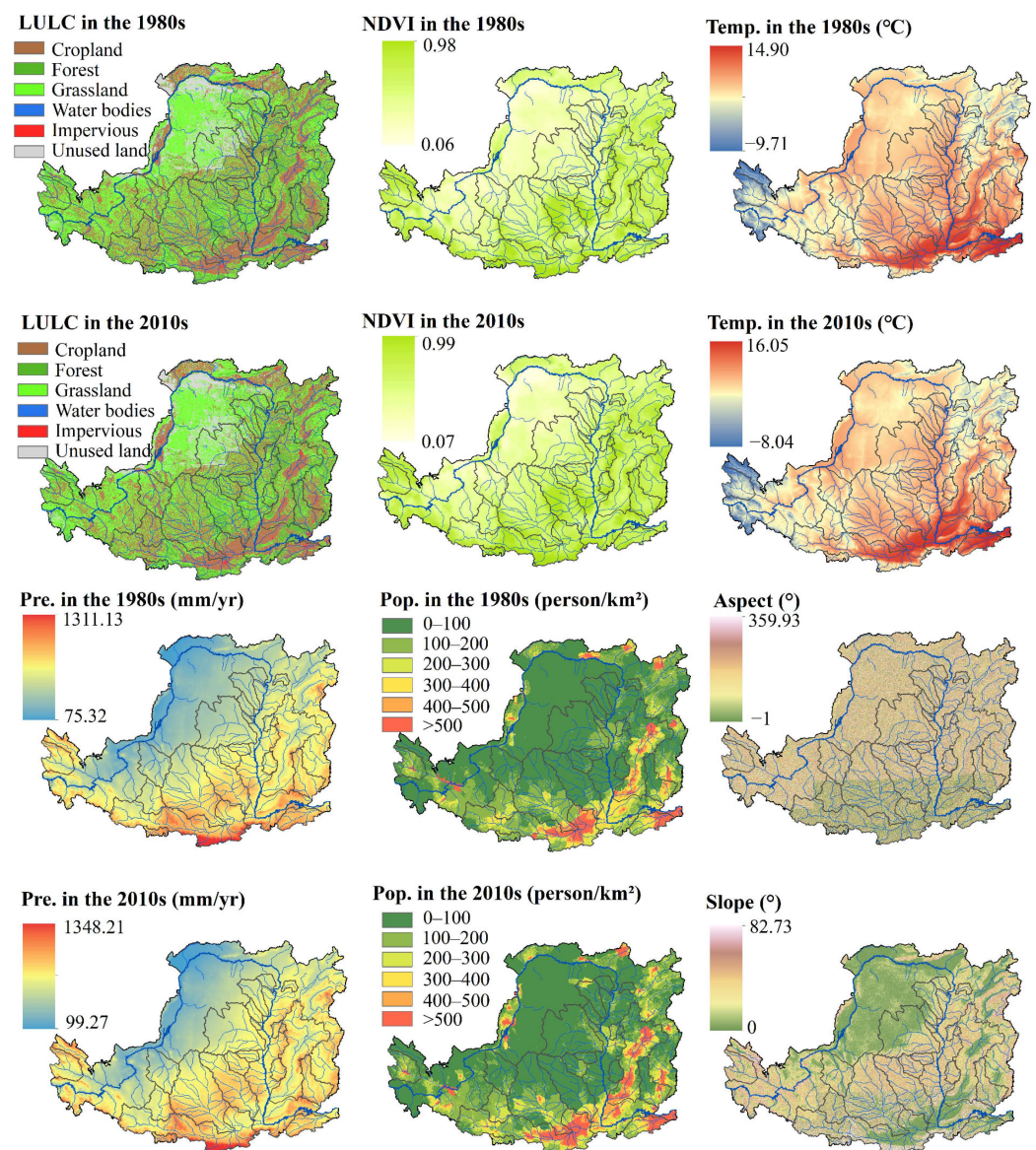


Figure 2. Spatial distributions of different impact factors in the 1980s and 2010s. Temp.—air temperature (°C); Pre.—annual precipitation (mm/yr); Pop.—population density (person/km²).

4. Results

4.1. Ecological Environment Characteristics

The comparative results of ecological environment indicators in different basins of the Loess Plateau are illustrated in Figure 3. The spatial variations of precipitation in the 1980s and 2010s were similar, exhibiting a spatial pattern of west < north < southwest

< southeast (Figure 3a). For instance, the mean precipitation in the Huangshui and Qingshui River basins in the west was 535.51 mm and 339.95 mm in the 1980s, with a significant difference of 195.56 mm. In contrast, in the southwestern and southeastern basins, the mean precipitation during the 1980s ranged from 509.93 mm to 617.08 mm and from 524.90 mm to 686.00 mm, respectively. There was also a significant spatial variability in air temperature, with the lowest values occurring in the western Huangshui basin and the highest in the southeastern Yi basin in the 1980s and 2010s (Figure 3b). Population density exhibited a relatively weak spatial heterogeneity, with the most significant differences observed in the southeastern basins (Figure 3c). The spatial pattern of vegetation coverage showed a gradient of north < west < southwest < southeast. Moreover, the mean NDVI for the western, northern, southwestern, and southeastern basins was 0.49, 0.44, 0.54, and 0.67 in the 1980s, respectively (Figure 3d).

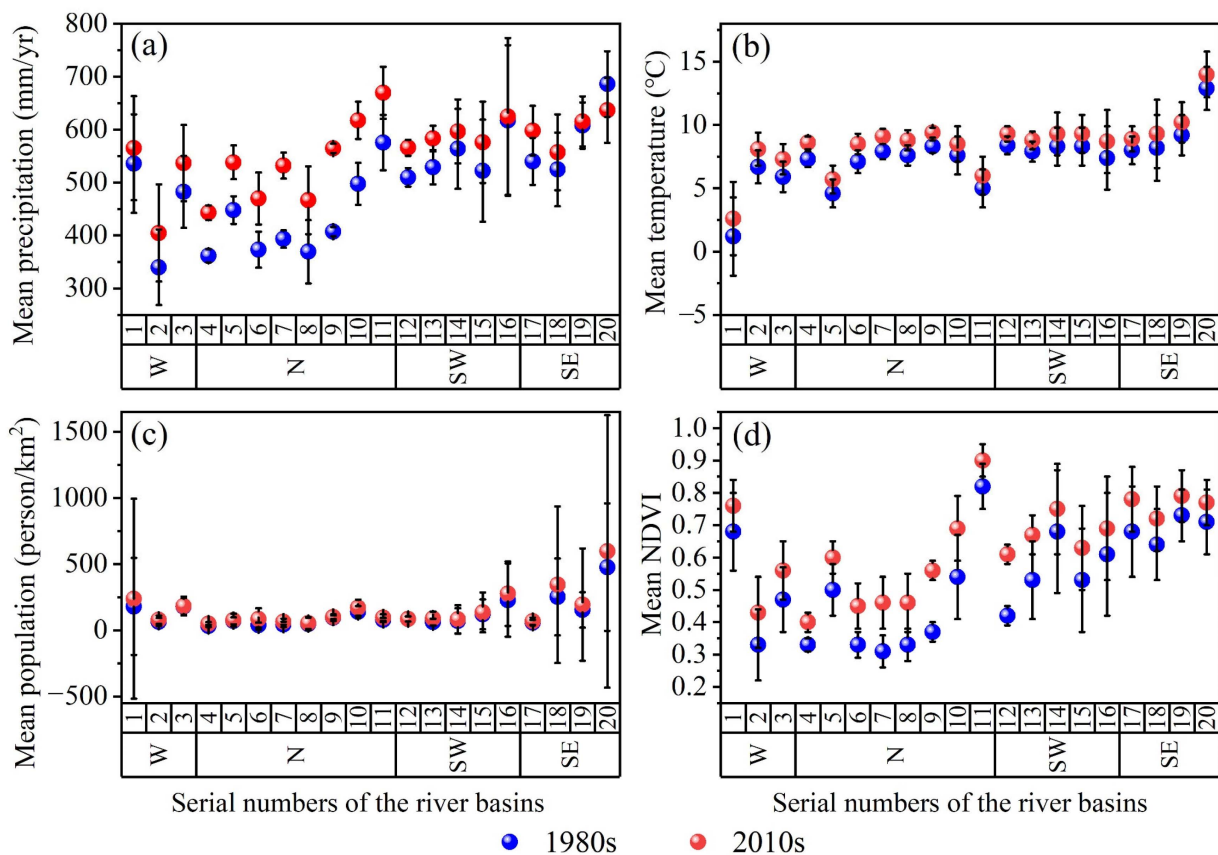


Figure 3. The comparisons of mean (a) precipitation, (b) temperature, (c) population density, and (d) NDVI in the 1980s and 2010s for different river basins (Table 1). W—the western part; N—the northern part; SW—the southwestern part; SE—the southeastern part.

From a temporal perspective, the basins in the Loess Plateau showed increasing trends in precipitation, air temperature, population density, and vegetation coverage from the 1980s to the 2010s. With the exception of the Yi River basin, all other basins witnessed increases in precipitation from 7.47 to 157.37 mm (Figure 3a), particularly the northern basins. For instance, the Jialu River basin experienced a 157.37 mm increase in rainfall during the 1980s to the 2010s. The air temperature in different basins increased by 0.87 to 1.47 °C from the 1980s to the 2010s, and the increased magnitudes were relatively consistent across different basins (Figure 3b). The increase in population density during the 1980s to the 2010s occurred mainly in the southeastern basins (Figure 3c). For example, the population density in the Yi River basin increased by 119 persons/km². The NDVI of different basins increased by 0.06–0.19 from the 1980s to the 2010s. Mean NDVI ranged from 0.06 to 0.98 in the 1980s and from 0.07 to 0.99 in the 2010s, with a mean growth

rate of 0.0036/yr. Moreover, the northern basin exhibited the most significant growth (Figure 3d). For example, the northern Jialu River basin saw an increase in NDVI from 0.37 to 0.56 from the 1980s to the 2010s.

4.2. Spatial Variations in SPS

The mean SPS at different hydrological stations in the Loess Plateau is shown in Figure 4. The spatial distribution characteristics of SPS in the 1980s and 2010s were similar, with coarse particles predominantly found at the northern stations and fine particles at the southern stations. SPS at the Wenjiachuan, Zhaoshiyao, and Shenjiawan stations in the northern Kuye, Wuding, and Jialu river basins was mostly concentrated in the 30–80 μm range, with mean values reaching up to 46 μm . More specifically, during the 1980s, SPS increased sequentially in the western, southeastern, southwestern, and northern basins, presented respective SPS ranges of 15–21, 11–34, 24–30, and 32–82 μm , and had mean values of 20, 24, 27, and 49 μm , respectively (Figure 4a). In the 2010s, stations with fine particles were mainly situated in the southwestern basins, with mean SPS generally ranging from 6 to 28 μm (Figure 4b). Stations with intermediate SPS were primarily situated in the southeastern part, particularly within the Fen River basin, where SPS mostly fell between 28 and 73 μm with a mean size of 24 μm . In comparison, SPS was high in the northern basins and low in the western basins during the 1980s, while in the 2010s, SPS was high in the northern basins and low in the southwestern basins. Consequently, the spatial pattern of SPS underwent changes during the 1980s to the 2010s, especially in the river basins located in the southwestern and southeastern regions of the Loess Plateau.

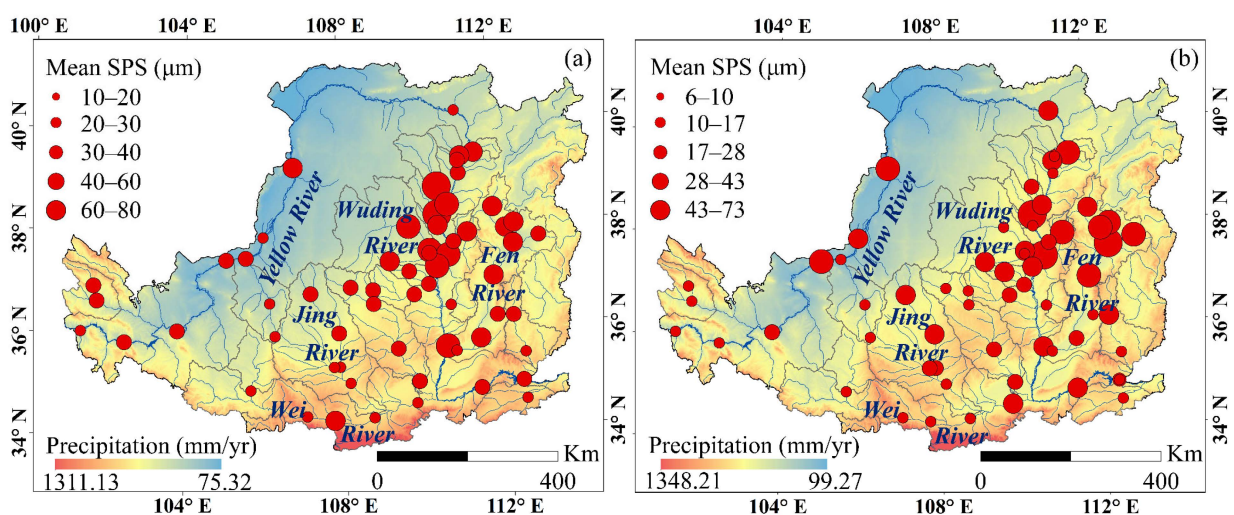


Figure 4. Mean SPS values at different hydrological stations in the (a) 1980s and (b) 2010s.

4.3. Temporal Variations in SPS

Except for a few basins in the northern and southeastern regions, mean SPS significantly decreased in most of the 20 tributary basins of the Yellow River during the 1980s to the 2010s. The basin-based mean SPS across the entire Loess Plateau ranged from 11 to 85 μm in the 1980s, with a mean value of 33 μm . In the 2010s, the basin-based mean SPS ranged from 6 to 73 μm , with a mean value of 20 μm (Figure 5). From the 1980s to the 2010s, the mean SPS in the northern Pianguan River basin increased from 41 μm to 43 μm , reflecting a 4.9% increase; the mean SPS in the southeastern Yi River basin remained relatively stable, with mean values of 11 μm during both periods (Figure 5). In contrast, the mean SPS in other basins exhibited reductions, primarily falling within the range of 0 to 26 μm . From the 1980s to the 2010s, the mean reductions of SPS in the northern, western, southwestern and southeastern basins were 42.0%, 29.4%, 46.3%, and 36.8%, respectively. In other words, the most pronounced particle size refinement was observed in the northern and southwestern parts of the Loess Plateau. Notably, the Kuye, Wuding, and Jialu river

basins in the northern region experienced the most significant refinement in SPS, with reductions ranging between 27 to 73 μm and reduction rates of 77.5%, 61.1%, and 83.7%, respectively (Figure 5).

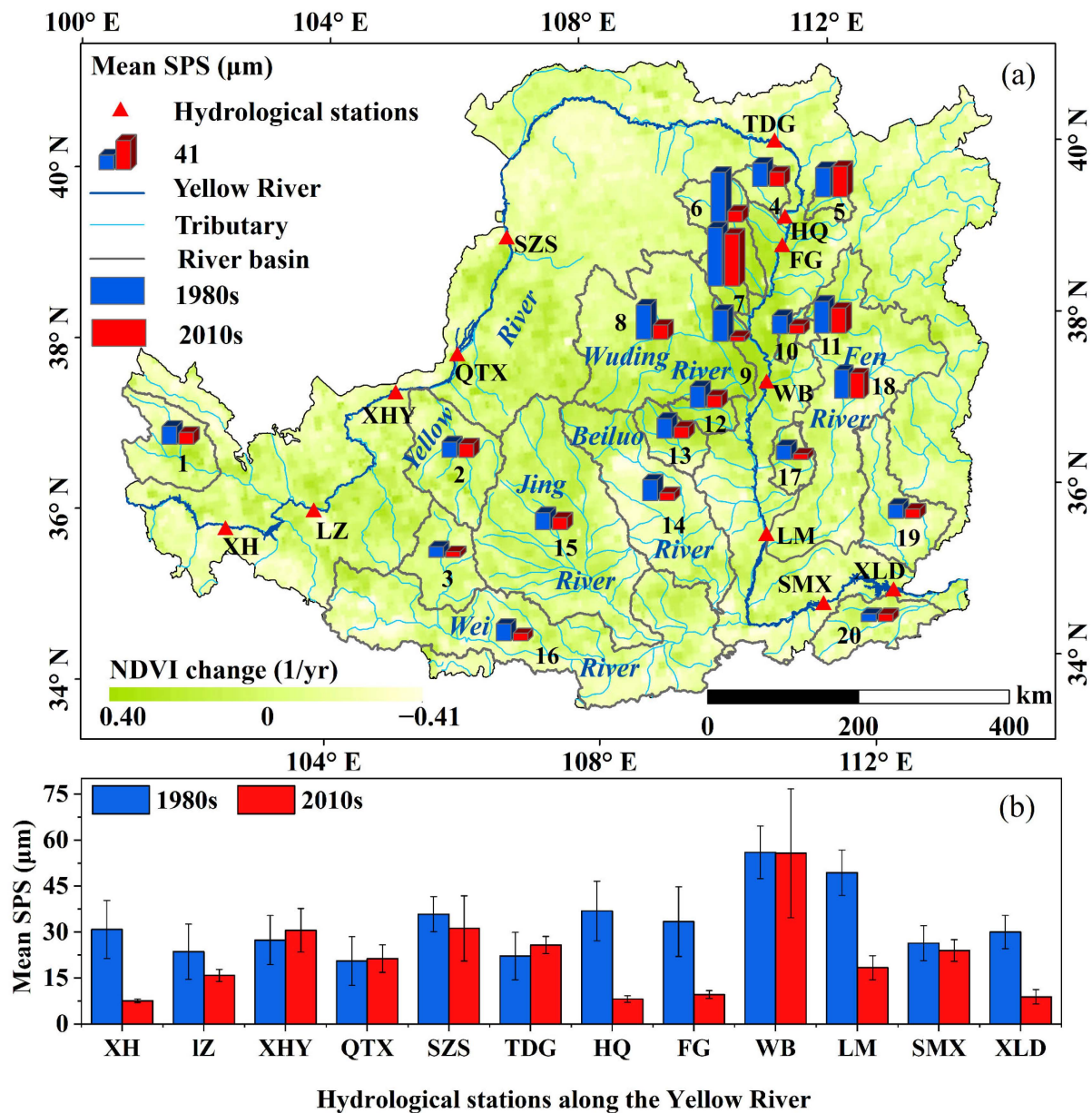


Figure 5. (a) The comparisons of mean SPS values for different river basins in the 1980s and 2010s. Mean SPS is the arithmetic average value of SPS at all hydrological stations in a specific river basin. (b) The comparisons of mean SPS values for different hydrological stations in the Yellow River mainstream.

This study also compared the cumulative volume percentage curves of SPS at different hydrological stations across the Loess Plateau in the 1980s and 2010s. Among the 54 hydrological stations with SPS spectrum data, 34 stations exhibited a trend of decreasing SPS from the 1980s to the 2010s; 12 stations showed no significant changes; and the remaining eight stations experienced an increase. Moreover, the temporal variations in SPS during the 1980s to the 2010s were inconsistent across different basins. For example, the cumulative volume percentages for various SPS classes increased at all four hydrological stations in the Wuding River basin (8-1/2/3/4) but showed a decreasing trend in the Beiluo River basin (14-1/2/3/4/5) (Figure 6). The changes in SPS at different hydrological stations

within a specific basin also showed differences from the 1980s to the 2010s. For the Yellow River, the cumulative volume percentage at the Hequ station (21-7) increased for all SPS classes, remained relatively stable at the Qingtongxia station (21-4), but decreased at the Xiaolangdi station (21-12). The spatial differences in the variability of SPS during the 1980s to the 2010s collectively reflected the differences in the influencing factors.

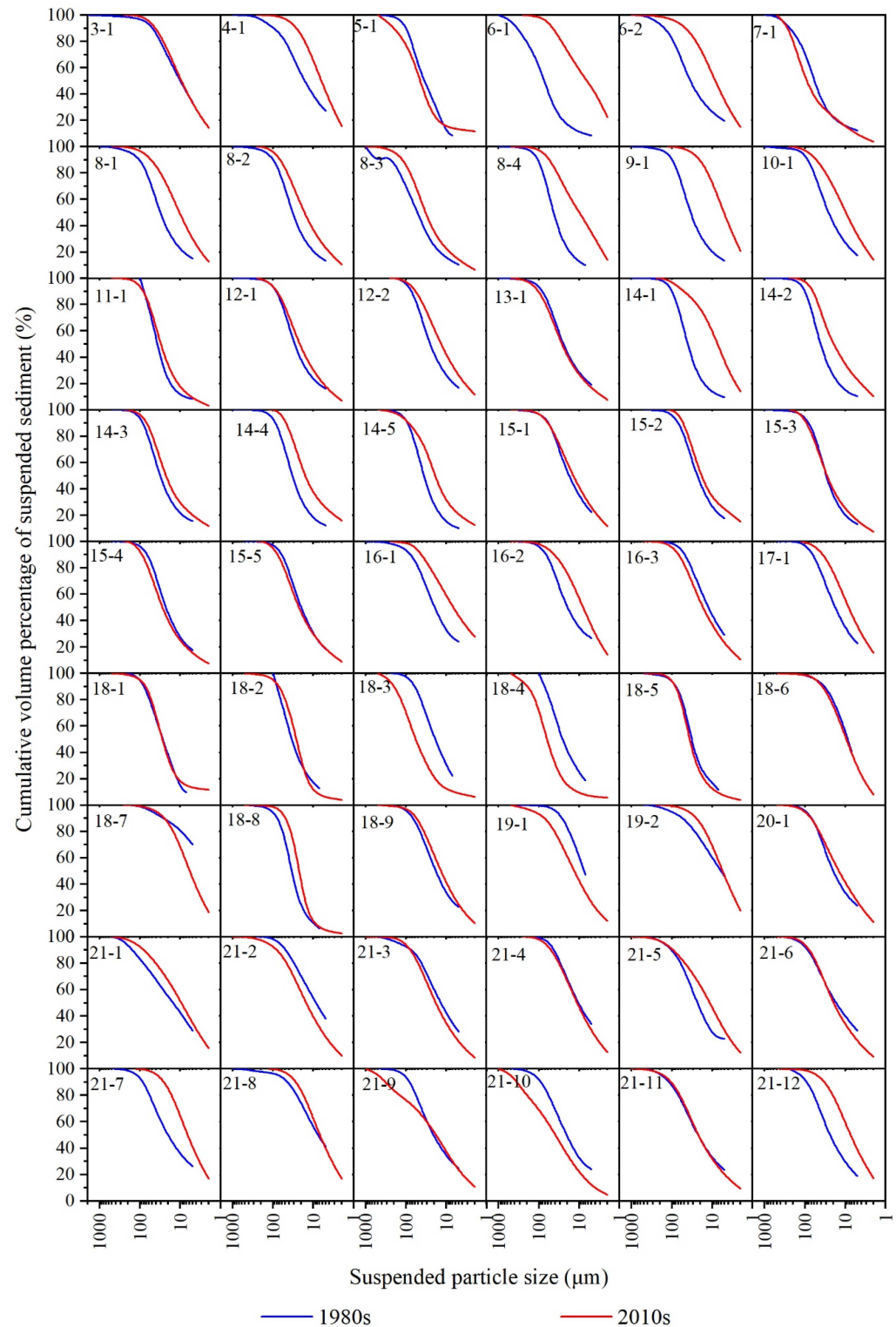


Figure 6. The cumulative volume percentage curves of different SPS in the 1980s and 2010s. Please refer to Table A1 for the names of river basins and hydrological stations.

4.4. Relative Importance of the Affecting Factors

The correlation analysis results between SPS and driving factors such as human management, meteorological and hydrological conditions, and topographical features are illustrated in Figure 7. In the 1980s, the SPS exhibited a significant negative correlation with slope, precipitation, population density, and NDVI, with Pearson’s r values of -0.54 , -0.53 , -0.50 , and -0.46 , respectively (Figure 7a). The relationship between slope aspect and SPS was positively correlated, but the correlation was not significant ($p > 0.05$). In the 2010s, although SPS still exhibited a negative correlation with slope, precipitation, population density, and NDVI, none of these correlations were significant (Figure 7b). These changes indicated that the influencing factors of SPS in the Loess Plateau have changed from the 1980s to the 2010s, along with climate and human activities.

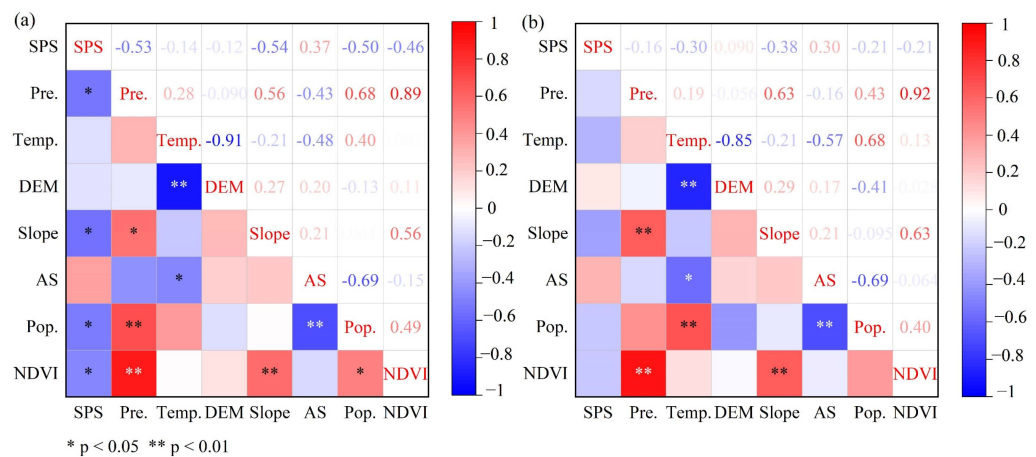


Figure 7. The Pearson’s r values between mean SPS and impact factors for different river basins in the (a) 1980s and (b) 2010s. The symbol “***” indicates $p < 0.01$; the symbol “**” denotes $p < 0.05$. In the analysis, we excluded the 13 hydrological stations in the Yellow River mainstream, whose SPS values were co-determined by the suspended sediment from the tributaries.

Regression analysis indicated that the selected influencing factors significantly affected the spatial distribution of SPS in the Loess Plateau during the 1980s ($p < 0.05$). In the 1980s, topography, landform (slope), and human factors (population density, NDVI, and land use) were the primary drivers of the spatial variation in SPS; these factors explained 25.7%, 25.9%, and 24.0% of the spatial variability, respectively. In the 2010s, the explanatory power of topographic slope for SPS variability decreased by 16.6%, and other natural factors no longer exhibited significant impacts on SPS variability ($p > 0.05$) (Figure 8).

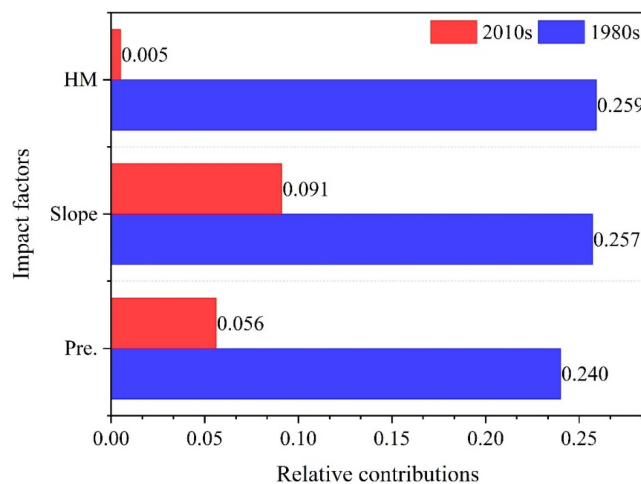


Figure 8. The comparisons of relative contributions of each impact factor in the 1980s and 2010s.

5. Discussion

5.1. Driving Forces to the Spatiotemporal Variations

The results showed that the mean SPS in the Loess Plateau Rivers decreased from 33 μm to 20 μm from the 1980s to the 2010s, and the SPS decreased significantly in all basins except for the pianguan and Yi River basins. We additionally collected the median SPS data from 14 hydrological stations for the 2020s (2018–2022) and compared them with the 1980s; we found that the SPS was still decreasing at 93% of the stations (Figure A1). The SPS in the Loess Plateau rivers results from a combination of natural factors and human activities in the watershed [12]. Since the 1980s, a series of soil and water conservation measures have been implemented in the Loess Plateau, including optimizing land use structure, terracing, reforestation, recovering ecology, and constructing a reservoir [20]. These activities have significantly altered sediment discharge in the Loess Plateau rivers [29] and have had considerable impacts on SPS distribution. In other words, human activities have gradually reduced the dominant role of natural factors in the SPS variability.

5.1.1. Topography and Landform

The slope was a key factor determining the surface runoff and soil erosion. Canton et al. [30] noted that sediment yield significantly increased with increasing slope angles. This mechanism is attributed to the direct influence of slope on gravitational erosion, where a steeper slope often results in greater erosion. Regarding the SPS on steep slope basins in the Loess Plateau, Guo et al. [31] pointed out that gravitational erosion might have accounted for a significant portion of total erosion, leading to a reduction in the median SPS from 84 to 51 μm as gravitational erosion increased. Additionally, the slope aspect (direction) could also influence the SPS distribution by affecting sediment transport pathways. Overall, topographical factors significantly influenced the SPS in the Loess Plateau rivers by affecting factors such as water flow velocity, erosion intensity, sediment transport pathways, and mixing. Moreover, these influences have been corroborated in various case studies, highlighting the significance of topography in governing the SPS.

5.1.2. Atmospheric Precipitation

The specific effects of precipitation on SPS are moderated by a complex relationship between precipitation characteristics. The amount of precipitation is one of the factors, and for the same site, the percentage of SPS larger than 0.05 mm decreases rapidly and reaches a minimum when heavy rainfall occurs [32], which may be attributed to the fact that an increase in the amount of precipitation increases the velocity and scouring capacity of the water body, resulting in smaller particles being more easily suspended [33], whereas, when the amount of precipitation increases further until it exceeds a certain range, the percentage of suspended sand with particle size larger than 0.05 mm increases rapidly [32]. In addition, the variation in SPS is not solely determined by the amount of basin precipitation but is also related to other precipitation characteristics. Wang et al. [34] pointed out that the coarsening of SPS was also related to the relatively high frequency of hyper-concentrated flows. Lin et al. [35] noted that in some cases, the kinetic energy of the rainfall transient has a significant effect on the SPS. Furthermore, Liu and Lu [36] pointed out that there was also a trend of increasing suspended sediment content with SPS > 50 μm along with the increased seasonal variation rate of rainfall (p^2/P , p^2 —average rainfall in the wettest month, P —multi-year average rainfall). Therefore, when considering the impact of precipitation characteristics on SPS, it is essential to take into account not only total precipitation but also parameters like the seasonal variation rate and unevenness coefficient.

5.1.3. Human Management

Human activities significantly also impacted the spatiotemporal variability of SPS in the Loess Plateau rivers. The coarse particles at several hydrological stations were largely attributed to human mining activities. For example, more than forty state-owned coal mines and over three hundred small-scale coal mines are in the Wuding River basin, leading

to coarse SPS [37]. To protect the ecological environment of the Loess Plateau, the Chinese government has implemented a series of soil and water conservation measures since the 1980s, including converting marginal croplands to forests and grasslands, constructing terraces, and installing silt dams. These efforts resulted in reduced erosion of coarse sediment particles and further led to a reduction in the riverine SPS [11]. Additionally, human activities also decreased riverine SPS by altering land use in the Loess Plateau. In the 1980s, riverine SPS in the unused land was significantly coarser than in other land use types, and the cultivated land areas exhibited the smallest mean SPS (Table 2). In the 2010s, rivers in the forested and grassland areas had significantly larger SPS than those in the cultivated land areas. Moreover, there were significant differences in the mean SPS for different land use types in the 1980s ($p < 0.05$); however, there was no significant difference in the 2010s.

Table 2. Statistics of SPS under different land use types. Note: SD is the standard deviation; CV is the coefficient of variation.

Periods	LULC	Basins	Suspended Particle Size (μm)		
			Mean/ μm	SD	CV
1980s	Grassland	4	36	0.022	61.1%
	Forest	2	37	0.011	29.7%
	Cropland	13	29	0.010	34.5%
	Unused land	1	82	-	-
2010s	Grassland	10	24	0.019	79.2%
	Forest	2	24	0.015	62.5%
	Cropland	8	014	0.007	5.0%

Population density and NDVI were both negatively correlated with SPS (Figure 7), which indicated that human management reduced SPS in the Loess Plateau rivers. The SPS fining is closely related to human activities such as soil and water conservation and reservoir construction [11]. Terracing involves land levelling and the reduction of slope length to control soil erosion and sediment transport, ultimately reducing the SPS of sediment entering the rivers [38]. Reforestation involves increasing vegetation cover, which helps intercept rainfall and reduce the splashing effect of raindrops, ultimately preventing the erosion of coarse particles [39]. Silt ponds and reservoirs play a “trap coarse and discharge fine particle” role and can decrease SPS by reducing the frequency of high-sediment-laden water flow [40]. For instance, after the operation of large-scale reservoirs such as the Three Gorges, Xiangjiaba, and Xiaolongtan, the sediment transport in the upper reaches of the Yangtze River has shown a significant decreasing trend, accompanied by a continuous decrease in the median particle size of suspended sediment [40]. In summary, human management resulted in finer particles in the Loess Plateau rivers by reducing soil erosion and sediment transport.

5.2. Enlightenments to the Ecological Environment in the Loess Plateau

5.2.1. River Sedimentation

The SPS is a crucial influencing factor on the settling velocity of suspended sediment. For the lower reaches of the Yellow River, Xu et al. [41] demonstrated that sediment deposition was more reliant on coarse sediment particles, and the amount of deposition increased along with increasing SPS. Lin et al. [35] noted that finer particles are preferentially moved during sediment transport while coarser particles are preferentially deposited. In addition, persistent dry seasons would lead to severe channel shrinkage in the lower Yellow River and seriously threaten flood control and disaster prevention efforts. The Chinese government initiated the water and sediment regulation project for the Xiaolangdi Reservoir to reduce flood risk in 2002 [42]. The specific measures involve using the reservoir to trap coarse particles, adjusting the morphological characteristics of sediment deposition within the reservoir area, and transporting fine particles out to the ocean; these measures

can reduce sediment accumulation in the downstream river and prevent further lifting of the Yellow River's downstream riverbed [43]. Furthermore, Xu et al. [41] pointed out that erosion and sediment control measures could yield the best results in reducing sediment deposition for rivers with SPS > 50 μm .

5.2.2. Water Environment Quality in Rivers

The SPS in rivers also impacts water quality levels, including dissolved oxygen, turbidity, pH, and the transport of nutrients and heavy metals. First, suspended sediment provides essential organic and inorganic materials required for the functioning of aquatic ecosystems and supports the survival and ecological processes of biota [44]. Kellner [44] pointed out that fine particles, especially those <2000 μm in size, can have a more persistent impact on water quality and the health of aquatic ecosystems. For instance, due to their higher chemical reactivity, finer particles may have surfaces with higher organic content compared to coarser particles. The in-situ decomposition of these fine particles can deplete dissolved oxygen levels in water, leading to severe oxygen deficiency [45]. Similarly, some aerobic heterotrophic microorganisms and reducible inorganic ions are more prone to adsorb onto the surfaces of fine-grained suspended particles [46]. The biological degradation of organic matter and the redox reactions of inorganic ions both contribute to oxygen consumption. When dissolved oxygen decreases to a certain level, it may pose a threat to the biological communities in the water. Some oxidation reactions may be associated with acidic reactions that can lead to a decrease in water pH. In addition, SPS increases water turbidity by directly affecting the underwater light field, which in turn limits phytoplankton photosynthesis and primary productivity, and fine particles reduce water column light intensity [47]. The fine particles, while limiting the photosynthesis of phytoplankton, also alter the concentration of carbon dioxide in the water, potentially leading to a decrease in water pH.

Second, suspended sediment is a significant sorbent for nitrogen and phosphorus nutrients, with finer particles possessing large specific surface areas and strong adsorption capacities [48]. Previous studies indicated a close relationship between the speciation of nutrients in suspended particles and SPS [49]. Fine particles usually have high concentrations of weakly adsorbed phosphorus, organic phosphorus, and non-reactive organic phosphorus; coarse particles commonly contain elevated levels of detrital phosphorus and apatite phosphorus [50]. Third, suspended sediment particles also serve as important carriers for heavy metals in rivers. Yao et al. [51] pointed out that the concentrations of heavy metals generally increase as particle size decreases. For the Miami River, USA, Tansel and Rafiuddin [52] demonstrated that the contents of cadmium and mercury in fine-grained suspended sediment could be ten times higher than those in coarse-grained particles. In summary, smaller particles in suspended sediment are likely to result in stronger pollutant enrichments.

Total dissolved solids (TDS) are an aggregate measure of the amount of soluble components in a water body, including various metals, dissolved compounds, and salts mentioned earlier. SPS exerts complex effects on the content and distribution of TDS in water. Smaller suspended sediment particles typically have a larger surface area, allowing them to adsorb and enrich soluble substances in the water more effectively. Larger particles of suspended sediment are prone to settle at the bottom, thereby influencing TDS distribution in the water [10]. However, the relationship between suspended sediment particle size and TDS in the water is influenced by various factors, such as pH, ion strength, temperature, dissolved oxygen, and the effects of biological growth processes [10]. Therefore, determining the specific impact of suspended particles on TDS requires careful consideration of the environmental conditions.

5.2.3. Organic Carbon Transport to the Estuary

The SPS is also related to riverine organic carbon transport from rivers to the ocean. As the sixth-largest river in the world, the Yellow River transports 1.34×10^{12} g C/yr to the

ocean annually [53]. Xia et al. [54] demonstrated that the spatiotemporal variations of total organic carbon (TOC) in the Yellow River were negatively related to SPS, with $r = 0.75$ and $p < 0.01$. Zhang et al. [55] also showed that the TOC content in the suspended sediment of the Yellow River decreased with increasing SPS. Thus, the refinement of the SPS in the Yellow River might lead to an increase in TOC content, which in turn affect the dissolved oxygen, carbon cycling, and algal photosynthesis in marine ecosystems [51]. This may further lead to the proliferation of planktonic and benthic organisms, thereby affecting the structure and function of the entire ecosystem [56]. Additionally, the mineralization and decomposition of terrigenous organic carbon can deplete dissolved oxygen in the water and absorb solar radiation, inhibiting the photosynthesis of phytoplankton [57]. Therefore, quantifying riverine TOC input based on SPS variations is crucial for enhancing our understanding of global carbon cycling and assessing organic pollution in marginal seas.

6. Conclusions

This study aims to thoroughly investigate the spatiotemporal variations of SPS in the Loess Plateau rivers in the 1980s and 2010s and to shed light on the impacts of human management on SPS through multifaceted analyses. The spatial pattern of SPS in the Loess Plateau rivers remained relatively consistent between the 1980s and 2010s, with coarser particles predominantly distributed in northern rivers. However, a significant reduction in SPS was evident when viewed through the temporal dimension, with the mean value of SPS reduced by $13 \mu\text{m}$. In addition, we found that the influences of anthropogenic management, for example, a series of erosion control measures, had weakened the dominant role of natural factors in driving SPS changes. This study fills a gap in existing research and provides a new perspective for understanding the dynamics of SPS in the Loess Plateau rivers.

Author Contributions: Conceptualization, K.L. and D.L.; methodology, K.L., D.L. and Z.Q.; formal analysis, K.L. and D.L.; resources, K.L., D.L. and Z.Q.; data curation, K.L., D.L. and M.D.; writing—original draft preparation, K.L., D.L., Z.Q. and M.D.; writing—review and editing, K.L., D.L., X.W. and H.D.; supervision, D.L. and H.D.; funding acquisition, D.L. and H.D. All authors have read and agreed to the published version of the manuscript.

Funding: This study was funded by the National Natural Science Foundation of China (Grants #U2243205, #42271376, and #41901299), the Natural Science Foundation of Jiangsu Province (Grants #BK20220018 and #BK20181102), the Youth Innovation Promotion Association CAS (Grant #2021313), and the NIGLAS Foundation (Grant #E1SL002).

Institutional Review Board Statement: Not applicable.

Informed Consent Statement: Not applicable.

Data Availability Statement: Data available on request. Most data are contained within the article.

Acknowledgments: Acknowledgement for the data support from “National Earth System Science Data Center, National Science and Technology Infrastructure of China” (<http://www.geodata.cn> (accessed in December 2022 to June 2023)).

Conflicts of Interest: Author Xiaodao Wei was employed by the company Shanghai Investigation, Design & Research Institute Co., Ltd. The remaining authors declare that the research was conducted in the absence of any commercial or financial relationships that could be construed as a potential conflict of interest.

Appendix A

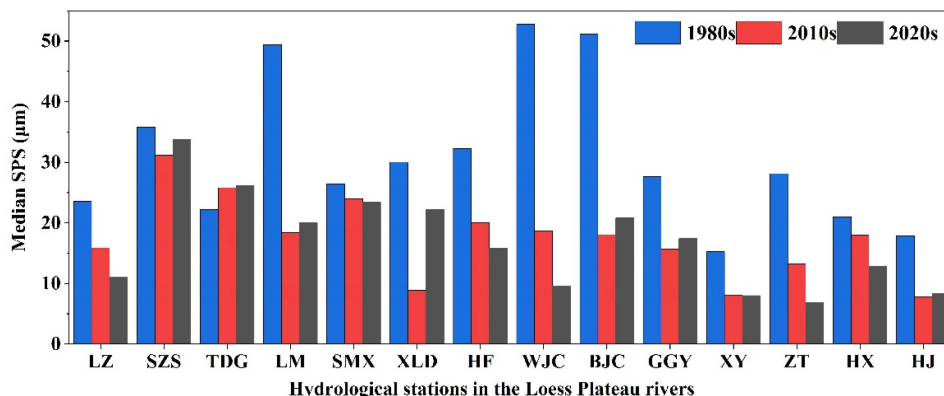


Figure A1. The comparison of median SPS in the Loess Plateau rivers during three periods.

Table A1. Names of river basins and hydrological stations. Min.—minimum value of SPS (µm); Max.—maximum value of SPS (µm); Mean—mean value of SPS (µm).

No.	River Name	No.	Hydrological Stations	Min	1980s Max	Mean	Min	2010s Max	Mean
1	Huang River	1-1	Xining	8	44	26	/	/	/
		1-2	Qiaotou	13	43	24	/	/	/
2	Qingshui River	2-1	Guyuan	9	21	16	/	/	/
		2-2	Hanfuwan	12	29	20	/	/	/
3	Hulu River	3-1	Qinan	6	31	15	4	17	8
		3-2	Huangfu	5	155	32	6	49	20
4	Pianguan River	4-1	Pianguan	12	68	41	26	56	43
		4-2	Shenmu	23	230	85	6	31	12
5	Kuye River	5-1	Wenjiachuan	11	110	53	5	78	19
		5-2	Gaojiachuan	39	185	82	11	183	73
6	Tuwei River	6-1	Dingjiagou	23	125	57	6	52	24
		6-2	Baijiachuan	25	99	51	7	47	18
7	Wuding River	7-1	Qingyangcha	6	94	37	4	128	26
		7-2	Suide	5	56	32	5	13	10
8	Jialu River	8-1	Zhaoshiyao	44	94	62	/	/	/
		8-2	Shenjiawan	6	125	43	5	24	7
9	Qiushui River	9-1	Linjiaping	10	82	26	6	23	13
		9-2	Beicuhan	13	148	45	26	47	35
10	Qingjian River	10-1	Zichang	6	75	32	6	48	21
		10-2	Yanchuan	8	53	28	7	23	12
11	Yan River	11-1	Ganguyi	6	50	28	5	22	16
		11-2	Wuqi	6	62	29	6	19	10
12	Beiluo River	12-1	Liujiache	6	57	30	5	21	11
		12-2	Jiaokouhe	6	51	26	6	24	12
13	Beiluo River	13-1	Zhuangtou	7	73	28	3	33	13
		13-2	Zhidan	7	86	31	6	20	11
14	Jing River	14-1	Yangjiaping	5	36	15	5	21	12
		14-2	Jingcun	7	63	23	3	21	8
15	Jing River	15-1	Hongde	7	60	30	17	35	28
		15-2	Qingyang	8	106	30	4	31	18
16	Wei River	16-1	Yuluoping	8	78	23	5	29	17
		16-2	Linjiacun	8	97	20	/	/	/
17	Wei River	17-1	Weijiabao	8	224	39	4	10	7
		17-2	Xianyang	5	43	15	4	15	8
18	Wei River	18-1	Huaxian	5	51	21	6	32	18
		18-2							

Table A1. Cont.

No.	River Name	No.	Hydrological Stations	Min	1980s Max	Mean	Min	2010s Max	Mean		
17	Xinshui River	17-1	Danling	5	37	20	5	15	9		
		18-1	Jingle	22	212	45	10	49	24		
		18-2	Zhaishang	12	69	38	23	80	39		
		18-3	Lancun	8	76	35	26	60	43		
		18-4	Fenheerba	7	98	37	38	77	58		
18	Fen River	18-5	Yitang	22	70	38	32	61	39		
		18-6	Chaizhuang	5	62	35	8	21	12		
		18-7	Hejin	3	44	18	6	18	8		
		18-8	Lujiazhuang	15	48	32	22	50	35		
		18-9	Dongzhuang	14	41	28	6	14	11		
19	Qin River	19-1	Feiling	8	43	27	7	40	20		
		19-2	Runcheng	6	27	12	5	7	6		
20	Yi River	20-1	Longmenzhen	6	20	11	11	11	11		
		21-1	Xunhua	6	83	31	6	11	8		
		21-2	Lanzhou	6	110	24	8	33	16		
		21-3	Xiaheyan	7	71	27	11	86	31		
		21-4	Qingtongxia	5	69	21	8	63	21		
		21-5	Shizuishan	8	64	36	9	84	31		
		21-6	Toudaoguai	5	73	22	10	50	26		
		21	Yellow River	21-7	Hequ	8	103	37	5	10	8
				21-8	Fugu	7	160	33	7	13	10
				21-9	Wubao	10	62	56	8	34	56
				21-10	Longmen	5	115	49	10	20	18
				21-11	Sanmenxia	6	51	26	5	47	24
				21-12	Xiaolangdi	2	79	30	5	10	9
21-13	Guide			/	/	/	7	16	11		

References

- Newcombe, C.P.; Macdonald, D.D. Effects of Suspended Sediments on Aquatic Ecosystems. *N. Am. J. Fish. Manag.* **1991**, *11*, 72–82. [[CrossRef](#)]
- Wilson, C.G.; Kuhnle, R.A.; Bosch, D.D.; Steiner, J.L.; Starks, P.J.; Tomer, M.D.; Wilson, G.V. Quantifying relative contributions from sediment sources in Conservation Effects Assessment Project watersheds. *J. Soil Water Conserv.* **2008**, *63*, 523. [[CrossRef](#)]
- Bogen, J. Monitoring grain size of suspended sediments in rivers. In *Erosion and Sediment Transport Programmes in River Basins*; IAHS Press: Wallingford, UK, 1992.
- Wass, P.D.; Leeks, G.J.L. Suspended sediment fluxes in the Humber catchment, UK. *Hydrol. Process.* **1999**, *13*, 935–953. [[CrossRef](#)]
- Walling, D.E.; Owens, P.N.; Waterfall, B.D.; Leeks, G.J.L.; Wass, P.D. The particle size characteristics of fluvial suspended sediment in the Humber and Tweed catchments, UK. *Sci. Total Environ.* **2000**, *251–252*, 205–222. [[CrossRef](#)]
- D'Sa, E.J.; Miller, R.L.; McKee, B.A. Suspended particulate matter dynamics in coastal waters from ocean color: Application to the northern Gulf of Mexico. *Geophys. Res. Lett.* **2007**, *34*, L23611. [[CrossRef](#)]
- Guo, C.; Jin, Z.; Guo, L.; Lu, J.; Ren, S.; Zhou, Y. On the cumulative dam impact in the upper Changjiang River: Streamflow and sediment load changes. *CATENA* **2020**, *184*, 104250. [[CrossRef](#)]
- Mohamadi, M.A.; Kaviani, A. Effects of rainfall patterns on runoff and soil erosion in field plots. *Int. Soil Water Conserv. Res.* **2015**, *3*, 273–281. [[CrossRef](#)]
- Struck, M.; Andermann, C.; Hovius, N.; Korup, O.; Turowski, J.M.; Bista, R.; Pandit, H.P.; Dahal, R.K. Monsoonal hillslope processes determine grain size-specific suspended sediment fluxes in a trans-Himalayan river. *Geophys. Res. Lett.* **2015**, *42*, 2302–2308. [[CrossRef](#)]
- Butler, B.A.; Ford, R.G. Evaluating Relationships Between Total Dissolved Solids (TDS) and Total Suspended Solids (TSS) in a Mining-Influenced Watershed. *Mine Water Environ.* **2018**, *37*, 18–30. [[CrossRef](#)]
- Sadeghi, S.H.; Gharemahmudli, S.; Kheirfam, H.; Khaledi Darvishan, A.; Kiani Harchegani, M.; Saeidi, P.; Gholami, L.; Vafakhah, M. Effects of type, level and time of sand and gravel mining on particle size distributions of suspended sediment. *Int. Soil Water Conserv. Res.* **2018**, *6*, 184–193. [[CrossRef](#)]
- Kellner, E.; Hubbart, J.A. Spatiotemporal variability of suspended sediment particle size in a mixed-land-use watershed. *Sci. Total Environ.* **2018**, *615*, 1164–1175. [[CrossRef](#)] [[PubMed](#)]
- Xu, L.; Zhang, D.; Proshad, R.; Chen, Y.-L.; Huang, T.-F.; Ugurlu, A. Effects of soil conservation practices on soil erosion and the size selectivity of eroded sediment on cultivated slopes. *J. Mt. Sci.* **2021**, *18*, 1222–1234. [[CrossRef](#)]

14. Attal, M.; Mudd, S.M.; Hurst, M.D.; Weinman, B.; Yoo, K.; Naylor, M. Impact of change in erosion rate and landscape steepness on hillslope and fluvial sediments grain size in the Feather River basin (Sierra Nevada, California). *Earth Surf. Dynam.* **2015**, *3*, 201–222. [[CrossRef](#)]
15. Gao, J.H.; Jia, J.; Wang, Y.P.; Yang, Y.; Li, J.; Bai, F.; Zou, X.; Gao, S. Variations in quantity, composition and grain size of Changjiang sediment discharging into the sea in response to human activities. *Hydrol. Earth Syst. Sci.* **2015**, *19*, 645–655. [[CrossRef](#)]
16. Liu, X.; Vandenberghe, J.; An, Z.; Li, Y.; Jin, Z.; Dong, J.; Sun, Y. Grain size of Lake Qinghai sediments: Implications for riverine input and Holocene monsoon variability. *Palaeogeogr. Palaeoclimatol. Palaeoecol.* **2016**, *449*, 41–51. [[CrossRef](#)]
17. Walling, D.E.; Moorehead, P.W. Spatial and Temporal Variation of the Particle-Size Characteristics of Fluvial Suspended Sediment. *Geogr. Ann. Ser. A Phys. Geogr.* **1987**, *69*, 47–59. [[CrossRef](#)]
18. Zhao, G.; Mu, X.; Wen, Z.; Wang, F.; Gao, P. Soil Erosion, Conservation, and Eco-Environment Changes in the Loess Plateau of China. *Land Degrad. Dev.* **2013**, *24*, 499–510. [[CrossRef](#)]
19. Zhuang, J.; Peng, J.; Wang, G.; Javed, I.; Wang, Y.; Li, W. Distribution and characteristics of landslide in Loess Plateau: A case study in Shaanxi province. *Eng. Geol.* **2018**, *236*, 89–96. [[CrossRef](#)]
20. Kong, D.; Miao, C.; Borthwick, A.G.L.; Lei, X.; Li, H. Spatiotemporal variations in vegetation cover on the Loess Plateau, China, between 1982 and 2013: Possible causes and potential impacts. *Environ. Sci. Pollut. Res.* **2018**, *25*, 13633–13644. [[CrossRef](#)]
21. Xu, J.X. Variation in grain size of suspended load in upper Changjiang River and its tributaries by human activities. *J. Sediment Res.* **2005**, *3*, 8–16.
22. Liu, X.; Feng, X.; Liu, J.; Lin, L. Laboratory application of laser grain-size analyzer in determining suspended sediment concentration. *J. Ocean Univ. China* **2014**, *13*, 375–380. [[CrossRef](#)]
23. Xie, J.; Liu, X.; Peng, B.; Liu, C. Rapid Watershed Delineation Using an Automatic Outlet Relocation Algorithm. *Water Resour. Res.* **2022**, *58*, e2021WR031129. [[CrossRef](#)]
24. Xu, X.L. *Spatially Interpolated Dataset of Average Conditions of Meteorological Elements in China*; Resource and Environment Science and Data Center: Beijing, China, 2017. [[CrossRef](#)]
25. Xu, X.L. *Annual 8 km Vegetation Index Dataset from 1981 to 2012 in China*; Resource and Environment Science and Data Center: Beijing, China, 2022. [[CrossRef](#)]
26. Xu, X.L.; Liu, J.Y.; Zhang, S.W.; Li, R.D.; Yan, C.Z.; Wu, S.X. *China Multi-Period Land Use Remote Sensing Monitoring Dataset (CNLUCC)*; Resource and Environment Science and Data Center: Beijing, China, 2018. [[CrossRef](#)]
27. Xu, X.L. *China Population Spatial Distribution Kilometer Grid Dataset*; Resource and Environment Science and Data Center: Beijing, China, 2017. [[CrossRef](#)]
28. Abdi, H. Coefficient of variation. *Encycl. Res. Des.* **2010**, *1*, 169–171.
29. Miao, J.; Zhang, X.; Zhao, Y.; Wei, T.; Yang, Z.; Li, P.; Zhang, Y.; Chen, Y.; Wang, Y. Evolution patterns and spatial sources of water and sediment discharge over the last 70 years in the Yellow River, China: A case study in the Ningxia Reach. *Sci. Total Environ.* **2022**, *838*, 155952. [[CrossRef](#)] [[PubMed](#)]
30. Canton, Y.; Sole-Benet, A.; de Vente, J.; Boix-Fayos, C.; Calvo-Cases, A.; Asensio, C.; Puigdefabregas, J. A review of runoff generation and soil erosion across scales in semiarid south-eastern Spain. *J. Arid Environ.* **2011**, *75*, 1254–1261. [[CrossRef](#)]
31. Guo, W.; Xu, X.; Zhu, T.; Zhang, H.; Wang, W.; Liu, Y.; Zhu, M. Changes in particle size distribution of suspended sediment affected by gravity erosion: A field study on steep loess slopes. *J. Soils Sediments* **2020**, *20*, 1730–1741. [[CrossRef](#)]
32. Xu, J.X. Complicated relationships between suspended sediment grain-size, water discharge and sediment concentration in tributaries of middle Yellow River. *Geogr. Res.* **2003**, *22*, 39–48.
33. Zhang, Y.; Liang, J.; Zeng, G.; Tang, W.; Lu, Y.; Luo, Y.; Xing, W.; Tang, N.; Ye, S.; Li, X.; et al. How climate change and eutrophication interact with microplastic pollution and sediment resuspension in shallow lakes: A review. *Sci. Total Environ.* **2020**, *705*, 135979. [[CrossRef](#)]
34. Wang, Z.; Ta, W. Hyper-concentrated flow response to aeolian and fluvial interactions from a desert watershed upstream of the Yellow River. *CATENA* **2016**, *147*, 258–268. [[CrossRef](#)]
35. Lin, J.; Zhu, G.; Wei, J.; Jiang, F.; Wang, M.-K.; Huang, Y. Mulching effects on erosion from steep slopes and sediment particle size distributions of gully colluvial deposits. *CATENA* **2018**, *160*, 57–67. [[CrossRef](#)]
36. Liu, A.X.; Lu, J.F. Relations between Grain-size of Suspended Sediments and River Basin Environment in the Middle Yellow River. *Acta Geogr. Sin.* **2002**, *57*, 232–237. [[CrossRef](#)]
37. Li, H.; Ji, H.; Shi, C.; Gao, Y.; Zhang, Y.; Xu, X.; Ding, H.; Tang, L.; Xing, Y. Distribution of heavy metals and metalloids in bulk and particle size fractions of soils from coal-mine brownfield and implications on human health. *Chemosphere* **2017**, *172*, 505–515. [[CrossRef](#)] [[PubMed](#)]
38. Wen, Y.; Gao, P.; Mu, X.; Li, M.; Su, Y.; Wang, H. Experimental Study on Landslides in Terraced Fields in the Chinese Loessial Region under Extreme Rainfall. *Water* **2021**, *13*, 270. [[CrossRef](#)]
39. Zhang, R.; Li, M.; Yuan, X.; Pan, Z. Influence of rainfall intensity and slope on suspended solids and phosphorus losses in runoff. *Environ. Sci. Pollut. Res.* **2019**, *26*, 33963–33975. [[CrossRef](#)] [[PubMed](#)]
40. Liu, J.; Zheng, H.; Shen, Y.; Xing, B.; Wang, X. Variation in sediment sources and the response of suspended sediment grain size in the upper Changjiang River Basin following the large dam constructions. *Sci. Total Environ.* **2023**, *904*, 166869. [[CrossRef](#)] [[PubMed](#)]

41. Xu, J.; Hu, C.; Chen, J. Effect of suspended sediment grain size on channel sedimentation in the lower Yellow River and some implications. *Sci. China Ser. E Technol. Sci.* **2009**, *52*, 2330–2339. [[CrossRef](#)]
42. Hou, C.; Yi, Y.; Song, J.; Zhou, Y. Effect of water-sediment regulation operation on sediment grain size and nutrient content in the lower Yellow River. *J. Clean. Prod.* **2021**, *279*, 123533. [[CrossRef](#)]
43. Tian, S.; Li, Z.; Wang, Z.; Jiang, E.; Wang, W.; Sun, M. Mineral composition and particle size distribution of river sediment and loess in the middle and lower Yellow River. *Int. J. Sediment Res.* **2021**, *36*, 392–400. [[CrossRef](#)]
44. Kellner, E.; Hubbard, J.A. Improving understanding of mixed-land-use watershed suspended sediment regimes: Mechanistic progress through high-frequency sampling. *Sci. Total Environ.* **2017**, *598*, 228–238. [[CrossRef](#)]
45. Jia, Z.; Liu, T.; Xia, X.; Xia, N. Effect of particle size and composition of suspended sediment on denitrification in river water. *Sci. Total Environ.* **2016**, *541*, 934–940. [[CrossRef](#)]
46. Astoreca, R.; Doxaran, D.; Ruddick, K.; Rousseau, V.; Lancelot, C. Influence of suspended particle concentration, composition and size on the variability of inherent optical properties of the Southern North Sea. *Cont. Shelf Res.* **2012**, *35*, 117–128. [[CrossRef](#)]
47. Storlazzi, C.D.; Norris, B.K.; Rosenberger, K.J. The influence of grain size, grain color, and suspended-sediment concentration on light attenuation: Why fine-grained terrestrial sediment is bad for coral reef ecosystems. *Coral Reefs* **2015**, *34*, 967–975. [[CrossRef](#)]
48. St Pierre, K.A.; St Louis, V.L.; Schiff, S.L.; Lehnher, I.; Dainard, P.G.; Gardner, A.S.; Aukes, P.J.K.; Sharp, M.J. Proglacial freshwaters are significant and previously unrecognized sinks of atmospheric CO₂. *Proc. Natl. Acad. Sci. USA* **2019**, *116*, 17690–17695. [[CrossRef](#)] [[PubMed](#)]
49. Wang, X.-Q.; Liu, Z.-C.; Miao, J.-L.; Zuo, N. Relationship between nutrient pollutants and suspended sediments in upper reaches of Yangtze River. *Water Sci. Eng.* **2015**, *8*, 121–126. [[CrossRef](#)]
50. Wei, J.-F.; Chen, H.-T.; Liu, Y.-L.; Shan, K.; Yao, Q.-Z.; He, H.-J.; Yu, Z.-G. Phosphorus Forms of the Suspended Particulate Matter in the Yellow Rive Downstream During Water and Sediment Regulation 2008. *Huanjing Kexue* **2011**, *32*, 368–374. [[PubMed](#)]
51. Yao, Q.; Wang, X.; Jian, H.; Chen, H.; Yu, Z. Characterization of the Particle Size Fraction associated with Heavy Metals in Suspended Sediments of the Yellow River. *Int. J. Environ. Res. Public Health* **2015**, *12*, 6725–6744. [[CrossRef](#)]
52. Tansel, B.; Rafiuddin, S. Heavy metal content in relation to particle size and organic content of surficial sediments in Miami River and transport potential. *Int. J. Sediment Res.* **2016**, *31*, 324–329. [[CrossRef](#)]
53. Liu, J.; Song, X.; Wang, Z.; Yang, L.; Sun, Z.; Wang, W. Variations of carbon transport in the Yellow River, China. *Hydrol. Res.* **2014**, *46*, 746–762. [[CrossRef](#)]
54. Xia, X.; Dong, J.; Wang, M.; Xie, H.; Xia, N.; Li, H.; Zhang, X.; Mou, X.; Wen, J.; Bao, Y. Effect of water-sediment regulation of the Xiaolangdi reservoir on the concentrations, characteristics, and fluxes of suspended sediment and organic carbon in the Yellow River. *Sci. Total Environ.* **2016**, *571*, 487–497. [[CrossRef](#)]
55. Zhang, L.J.; Wang, L.; Cai, W.J.; Liu, D.M.; Yu, Z.G. Impact of human activities on organic carbon transport in the Yellow River. *Biogeosciences* **2013**, *10*, 2513–2524. [[CrossRef](#)]
56. Vilmin, L.; Flipo, N.; Escoffier, N.; Rocher, V.; Groleau, A. Carbon fate in a large temperate human-impacted river system: Focus on benthic dynamics. *Glob. Biogeochem. Cycles* **2016**, *30*, 1086–1104. [[CrossRef](#)]
57. Assemany, P.P.; Calijuri, M.L.; Couto, E.d.A.d.; de Souza, M.H.B.; Silva, N.C.; Santiago, A.d.F.; Castro, J.d.S. Algae/bacteria consortium in high rate ponds: Influence of solar radiation on the phytoplankton community. *Ecol. Eng.* **2015**, *77*, 154–162. [[CrossRef](#)]

Disclaimer/Publisher’s Note: The statements, opinions and data contained in all publications are solely those of the individual author(s) and contributor(s) and not of MDPI and/or the editor(s). MDPI and/or the editor(s) disclaim responsibility for any injury to people or property resulting from any ideas, methods, instructions or products referred to in the content.